

Experimental investigation on the effect of fibre consistency on rheology of aqueous foams in pipe flow

Prakash Baranivignesh, Ari Jäsberg and Antti I. Koponen

VTT Technical Research Centre of Finland Ltd, P.O. Box 1603, 40101 Jyväskylä, Finland

ABSTRACT

Due to recent development of foam forming for making fibrous structures (instead of traditional water forming), understanding on the rheology of aqueous fiber foam has become a necessity. However, this topic has been almost completely neglected in the existing academic literature, and most basic questions remain unanswered. In this paper we present results on the effect of fiber consistency on the rheology of aqueous fiber foams. Hardwood (birch) fibers were used at mass consistencies of 2, 3, 4 and 5%. Air content was 70% and SDS was used as the surfactant. The measurements were performed with a pipe rheometer, as normal rheometer geometries are unsuitable for these materials. In addition to shear rheology, slip flow at the pipe walls was also studied. The viscosity behaviour of the foams followed accurately a power law with all consistencies. Flow index was $n \sim 0.4$ and it decreased slightly with increasing consistency. The consistency index K was linearly dependent on consistency. The interaction between the fibers is thus clearly weaker in foam than in pure water. The slip behavior was similar for all consistencies.

INTRODUCTION

During last ten years, foam forming has been studied intensively as an alternative to water forming for making both traditional and novel products from natural and man-made fibers^{1 2}. The advantages of foam forming include high uniformity of the obtained structures, possibility to include many types

of raw materials, and ability to make highly porous lightweight materials and layered structures. Moreover, foam forming is generally efficient in terms of raw material, energy, and water use. Besides foam forming, foam coating is currently also being developed³.

The advantages of foam foaming are based on the rheological properties of foams⁴. Foam forming is typically performed at an air content of 60–70%. In this region foams are generally pseudoplastic power law fluids, with a viscosity that is clearly higher than that of water. The high viscosity decreases the mobility of the fibers and the bubbles attach to the fiber walls reducing fiber entanglement and reflocculation. Forming foams have also often a yield stress which further decreases the mobility of fibers during the late stages of forming when the shear stresses are small. These key properties explain the improved homogeneity achieved with using foam as the transporting material instead of water.

There is a lack of academic rheological studies that would help understanding and developing form forming. The rheology of particle-laden foams has been studied mainly in the presence of small particles (such foams are called pickering foams) and there are few studies where the size of particles has been similar or bigger than the bubble size.

There are to date only two paper, by Jäsberg at al., considering the rheology of fiber foams^{5 6}. In these papers the effect of hardwood (birch) pulp fibers, smooth cellulosic man-made fibers and microfibrillated cellulose

(MFC) was studied at 2.0% consistency with air content of 70%. It was found that man-made fibers had no observable effect on the foam viscosity, whereas the MFC and pulp fibers increased the foam viscosity by 30% and 100%, respectively. Obviously, at a selected consistency, the effect of fibrous material on the foam rheology depends on the characteristic length scale of fibres as compared with the mean bubble size as well as on the surface chemistry and texture of fibres.

In addition to viscous behavior, (apparent) slip flow is another important aspect of foam rheology. Slip refers to the sliding motion of foam bubbles along a smooth wall. Slipping is due to foams creating at the walls a liquid film of a few micrometers thick. Bubble size and added materials may effect on the thickness of this film by interfering the flow of liquid from the foam to the pipe wall. Jäsberg et al. studied also slip flow and found that slip was slightly higher for pure aqueous foam when compared to MFC foams. The slip flow of birch fiber foams was 40% smaller when compared to aqueous foams.

Currently there are no studies on the effect of fiber consistency on foam rheology. This paper aims to start filling this gap. The foam rheology is investigated with a pipe rheometer, as use of normal rheometer geometries would be hardly possible. In addition to shear rheology, slip flow at the pipe walls and the average bubble size are measured for hardwood fiber mass consistencies of 2, 3, 4 and 5% for a wide range of flow rates.

MATERIALS AND METHODS

Fibers, surfactant and making the foam

Hardwood (birch) sheets with 1 mm length and 15–20 μm width cellulose fibres were used to prepare fibre suspensions at four fibre mass consistencies ($c = 2, 3, 4$ and 5%).

Desired mass of hardwood sheets were torn into smaller pieces and soaked in tap water for 24 hours to loosen up the fibres. In each experiment, a 40 L fibre suspension batch was prepared in a 150 L conical-bottomed mixing tank mounted with three baffles located at 120° from one another. Radial impeller with profiled blades was bolted to the bottom of the tank and connected to a variable speed drive. The mixing tank was equipped with a cooling jacket to maintain the fibre-foam suspension temperature at 25 °C.

Preparation of fibre-foam suspension involved three steps. In the first step, the presoaked fibre solution was disintegrated in the mixing tank. The time of pulping and impeller speed were varied between one to three hours and 650 to 1250 rpm, respectively, depending on the fibre consistency (with higher consistency the pulping time and the impeller speed were also higher). Once the fibres were well dispersed, the second step of the foam generation was started by adding 2.5 g/lit of SDS (sodium dodecyl sulfate, Sigma-Aldrich, 98.5% purity) to the mixing tank. The surface tension of the SDS solution was ca. 33 mN/m, and the viscosity was very close to that of water². Such relatively high quantity (slightly above the critical micelle concentration) of SDS was used to have a good stability for the foam; the half-life time of the fiber foams, defined as the time required by the foam to drain 50% of the weight of the initial conditioning liquid used in foam generation, varied between 4 min to 5.5 min. Fibre-foam suspension was thoroughly mixed for 30 minutes to break the larger bubbles and to obtain a relatively narrow bubble size distribution. Notice that in the later part of the foam making, in addition to tank mixing, the foam was also circulated through a pipe which was equipped with a specifically designed contraction block that created highly turbulent flow and where compressed air was

injected into the foam ⁷. Once the fibre foam attained the desired quality and density of 300 kg/m³ (air volume fraction 0.70), it was transported to the online measurement unit through a centrifugal pump.

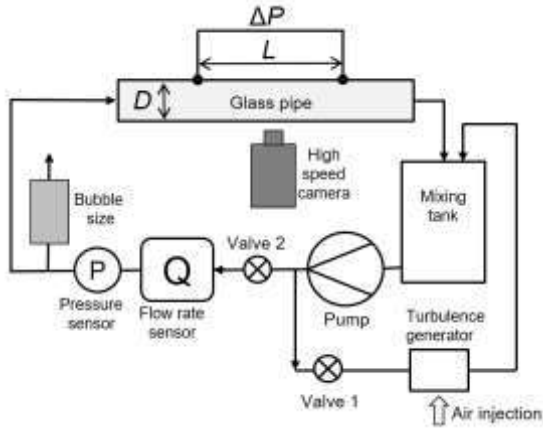


Figure 1 Schematic representation of the experimental setup.

Experimental setup for measuring foam rheology

A schematic diagram of the experimental facility used in the present study is shown in Figure 1. In the online measurement unit, located in the beginning of the flow loop, volumetric flow rate, absolute pressure and bubble size distribution were measured by a magnetic flow meter, pressure sensor and Pixact online foam monitoring device ⁸, respectively. Figure 2 shows two online foam images obtained with the Pixact device. Figure 3 shows examples of bubble size distributions. Notice that in foam-related applications, the surface weighted Sauter diameter ⁹

$$d = \frac{\sum_{i=1}^n n_i d_i^3}{\sum_{i=1}^n n_i d_i^2} \quad (1)$$

is generally used for the average bubble size

(above n_i is the number of bubbles having the diameter of d_i).

After the online measurement section, fibre-foam suspension flowed into a glass pipe of 2 m length and 0.015 m inner diameter where the pressure drop and foam motion were measured using a differential pressure transducer and a high-speed camera (HSC, 7000 fps), respectively. The distance of the first differential pressure transducer from the inlet of the pipe was more than 50 pipe diameters to achieve a fully developed flow. The obtained HSC images (see Figure 4 for examples) were processed using an in-house developed algorithm to calculate the slip velocity at the pipe wall.

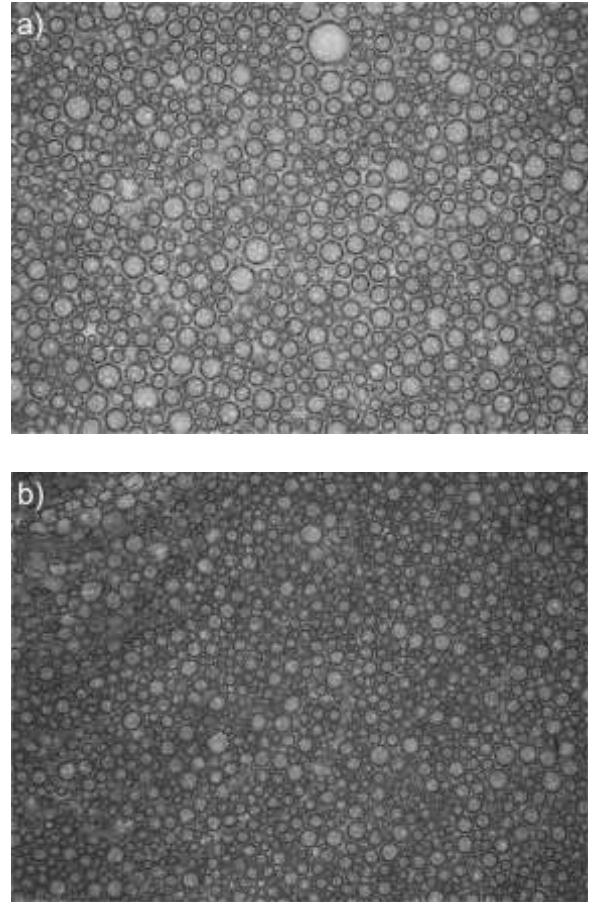


Figure 2 Images of fiber foams obtained with the Pixact foam monitoring system. The image size is 3.4 × 4.6 mm and pixel size is 3.2 μm. a) Fiber consistency is 2% b) Fiber consistency is 5%.

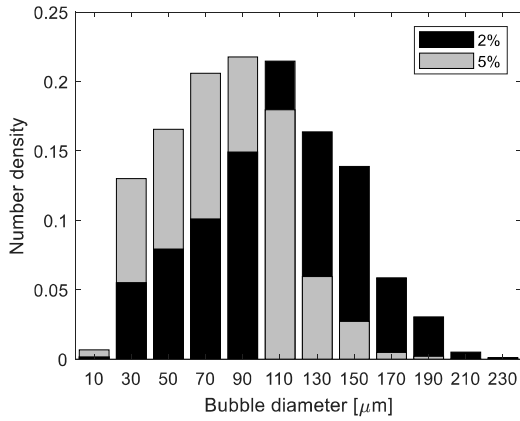


Figure 3 Examples of the measured bubble size distributions for 2% (Sauter diameter 135 μm) and 5% (Sauter diameter 103 μm) fiber foams

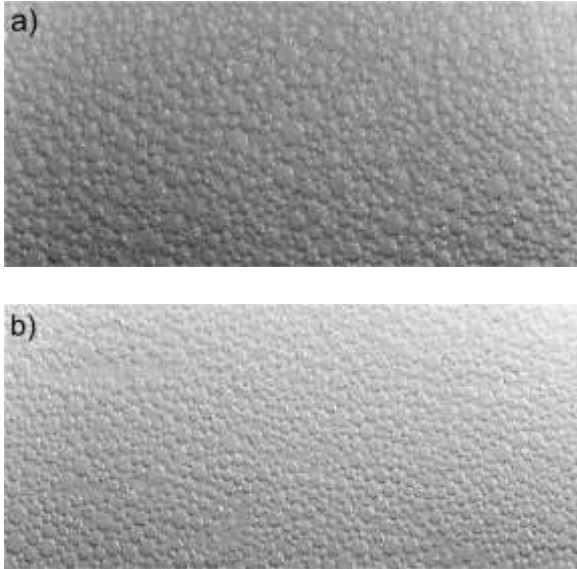


Figure 4 HSC images of fiber foams during flow in the pipe. The spatial size of the image is 15.4 mm \times 12.3 mm, and pixel size is 12 μm . a) Fiber consistency is 2% b) Fiber consistency is 5%

The volumetric flow rate varied at the magnetic flow meter between 2 – 12 lit/min. However, notice that due to declining pressure the foam expands when flowing from the volumetric flow measurement to the measurement pipe. As a consequence the volumetric flow rate increases. As the pressure P_o in the measurement pipe is close to the atmospheric pressure 101 kPa, the air

content φ at the pressure measurement point can be calculated from the formula

$$\varphi = \frac{P_o/P}{P_o/P + (1 - \varphi_o)/\varphi_o} \quad (2)$$

Above P is the measured pressure and $\varphi_o = 0.70$ is the air content of the foam in the atmospheric pressure. As the mass flow rate remains constant in the whole pipe, the volumetric flow rate Q_o in the measurement pipe can be obtained from the formula

$$Q_o = \frac{\rho}{\rho_o} Q \approx \frac{\rho_w(1 - \varphi)}{\rho_o} Q, \quad (3)$$

where Q is the measured volumetric flow rate, ρ is the density of the foam at the volumetric flow rate measurement point, ρ_o is the foam density at the atmospheric pressure, and $\rho_w = 1000 \text{ kg/m}^3$ is the density of water. Depending on the flow rate and consistency, the flow rate in the measurement pipe was 1.2-1.5 times higher than at the flow meter.

The bubble diameter d_o in the measurement pipe was calculated from the measured bubble size d using the equation

$$d_o = d \left(\frac{P}{P_o} \right)^{1/3} \quad (4)$$

obtained from the ideal gas equation. Above P is the pressure measured close to the bubble size measurement device and P_o is the atmospheric pressure.

Data analysis for rheology

For stationary flow in a circular pipe the wall shear stress is independent of the detailed flow profile and can be calculated from the measured pressure drop per unit length:

$$\tau_w = \frac{D}{4} \frac{dP}{dL}, \quad (5)$$

where D is the inner diameter of the pipe. In order to extract material parameters one has to examine the foam in the frame of reference moving at the speed of the slip velocity. To that end, the measured slip velocity v_s is subtracted from the mean flow velocity v_{avg}

$$v_{\text{bulk}} = v_{\text{avg}} - v_s. \quad (6)$$

Apparent foam shear rate $\dot{\gamma}_a$ at the edge of the foam plug is defined as

$$\dot{\gamma}_a = \frac{8v_{\text{bulk}}}{D}. \quad (7)$$

The real shear rate $\dot{\gamma}$ at the pipe wall can now be obtained by applying the Weissenberg-Rabinowitsch correction that takes into account the non-Newtonian features of the velocity profile^{10 11}:

$$\dot{\gamma} = \dot{\gamma}_a \times \frac{1}{4} \left(3 + \frac{d \ln \dot{\gamma}_a}{d \ln \tau_w} \right). \quad (8)$$

Foams are generally power law fluids; their viscosity is i.e. given with a good accuracy by the formula

$$\mu = K \dot{\gamma}^{n-1}, \quad (9)$$

where K is consistency index and n is flow index. The derivative $d \ln \dot{\gamma}_a / d \ln \tau_w$ is thus constant and equal to $1/n$. We calculate it by fitting a straight line through $(\ln \dot{\gamma}_a, \ln \tau_w)$ data points. Viscosity with a given shear rate is now obtained as the ratio of the wall shear stress to the real wall shear rate:

$$\mu = \tau_w / \dot{\gamma}. \quad (10)$$

Finally notice that we compare below the 2% fiber foam measurements performed by Jäsberg et al.⁵ with the present measurements. To be consistent we have recalculated the viscosity from the

measurement data of Jäsberg et al. by calculating $d \ln \dot{\gamma}_a / d \ln \tau_w$ from the linear fit.

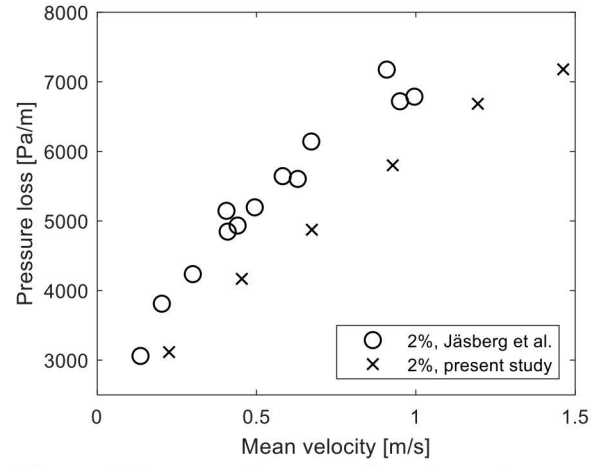


Figure 5 Pressure loss as a function of mean velocity with 2% fiber consistency for Jäsberg et al.⁵ and the present study.

RESULTS

Comparison with earlier measurements

Jäsberg et al.⁵ studied the effect of birch fibers on foam rheology at 2% consistency. Air content, foam temperature and SDS dosage were the same as in the present study. The measurement setups were different but the measurement glass pipes were identical.

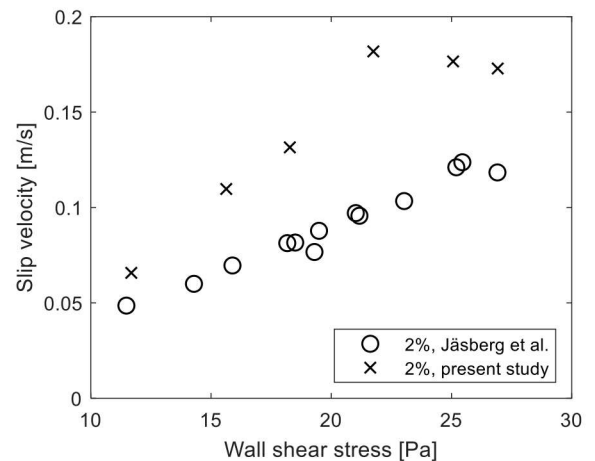


Figure 6 Slip velocity as a function of wall shear stress with 2% fiber consistency for Jäsberg et al.⁵ and the present study.

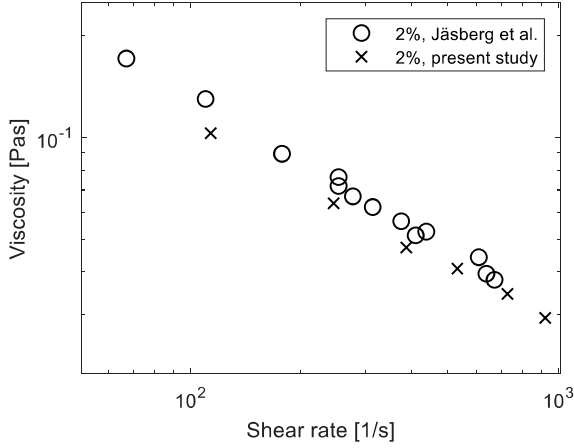


Figure 7 Viscosity as a function of shear rate with 2% fiber consistency for Jäsberg et al. ⁵ and the present study.

Figure 5 compares the pressure loss as a function of mean velocity obtained by Jäsberg et al. and in the current study. We see that with a given pressure loss the flow rate is in the present study clearly higher. This difference is mainly caused by the clearly higher slip velocity; see Figure 6. Figure 7 compares the fiber foam viscosities as a function of shear rate. In the shear rate region of 50 – 1000 1/s the viscosities of Jäsberg et al. are on the average 15% higher than in the present study.

The measurement conditions were similar in Jäsberg et al. and the present study. There may be some difference in the pressure level of the measurement pipe which could explain the small difference in the obtained viscosities. This difference could also be due to small differences in the used fiber batch or differences in the bubble size. The big difference in the slip velocities is likely due to the bubble size being in Jäsberg et al. smaller than in the current study ¹²; see below.

The effect of fiber consistency on the foam rheology

Figure 8 shows the pressure loss as a function of mean velocity for the four fiber consistencies. We see that the flow behaviour

is qualitatively quite similar for all consistencies and the pressure loss of the 5% foam is almost two times higher than for the 2% foam. The slip velocities are shown as a function of wall shear stress in Figure 9. We see that, perhaps surprisingly, slip is similar for all consistencies. The solid line in Figure 9 is a linear fit

$$v_s = (6.9\tau_w - 0.436) \times 10^{-3} \quad (11)$$

to all the data points.

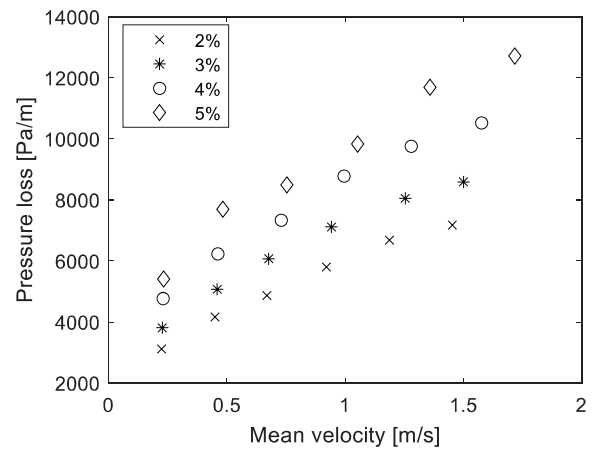


Figure 8 Pressure loss as a function of the mean velocity for different fiber consistencies.

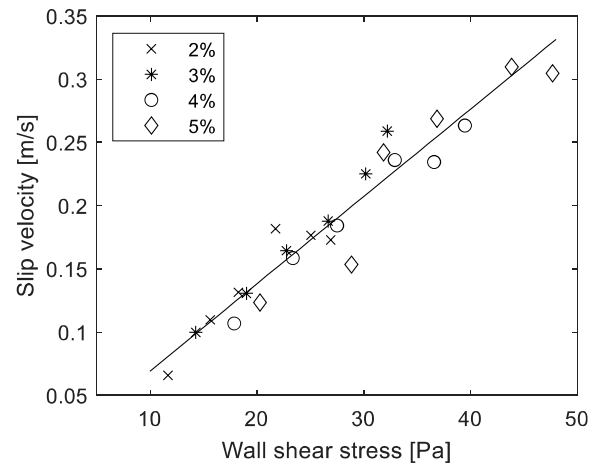


Figure 9 Slip velocity as a function of wall shear stress for different fiber consistencies. The solid line is a linear fit to all the data

points: $v_s = (6.9\tau_w - 0.436) \times 10^{-3}$.

Relative slip is defined as the quotient of slip velocity to the average velocity. We see in Figure 10 that in the measured flow rate range relative slip has always a significant contribution to the total flow and the contribution of slip increases with increasing consistency. The effect of slip becomes higher with lower wall shear stress (i.e. with lower flow rate). This is expected, as due to shear thinning the flow rate inside the pipe increases more rapidly than the slip flow when wall shear stress (i.e. pressure loss) increases.

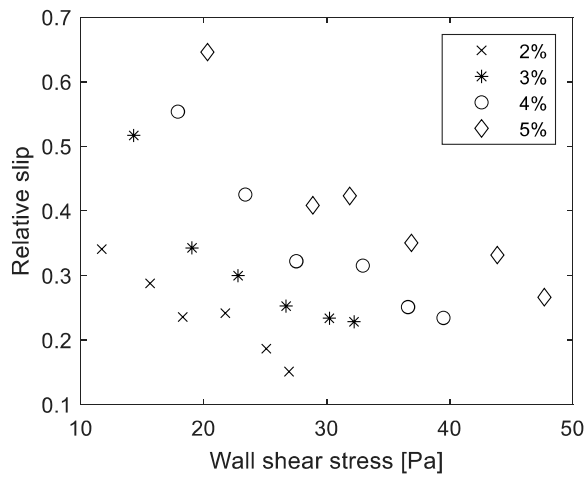


Figure 10 Relative slip velocity as a function of wall shear stress for different fiber consistencies.

The fiber foam viscosity is shown as a function of shear rate for different consistencies in Figure 11. The viscosity data for pure foam from Jäsberg et al. ⁵ is shown for comparison. The solid lines are fits of Eq. (9) to the data points. We see that in all the cases power law works very well for describing the viscous behaviour. We also see that the flow index is $n \sim 0.4$ but it decreases slowly with increasing consistency. The consistency index K is shown in Figure 12 as a function of consistency together with a fit of a linear function

$$K = 0.96c - 0.22 \quad (12)$$

to all the data points ($R^2=0.998$). The consistency index of fiber foams is thus linearly dependent on the consistency at least in the consistency range of 2% - 5%. Below 2% this linear trend must somewhere break; more measurement are here needed. The linear dependence reflects the low level of interaction between the fibers in foam. For water-fiber suspensions the dependence of the consistency index on consistency is expected to be a power law with an exponent of the order of 2-3 ¹³.

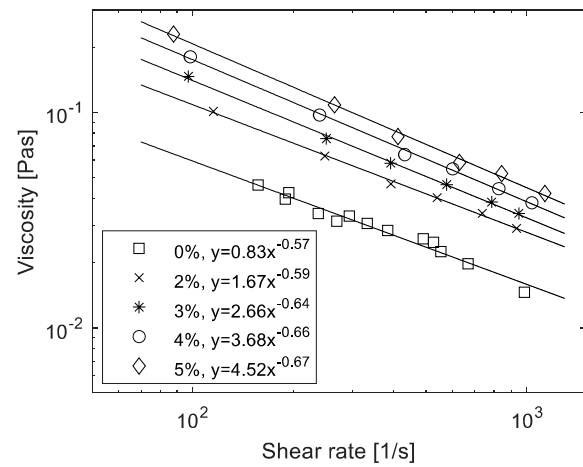


Figure 11 Viscosity of the foam as a function of shear rate for different fiber consistencies. Solid lines show a power law fit to the data points. The pure foam data is from Jäsberg et al. ⁵.

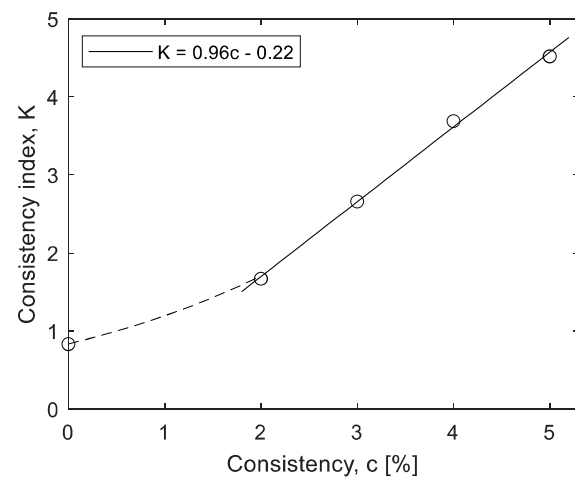


Figure 12 Consistency index K as a function of consistency.

The bubble size in the measurement pipe is shown in Figure 13 as a function of mean velocity. There are some exceptions, but generally bubble size remains almost constant with a fixed consistency and decreases with increasing fiber consistency. This is likely due to fibers increasing the shear forces acting on the bubble surfaces¹⁴. Notice that the bubble size in Jäsberg et al. varied between 90–110 μm for 2% fiber foam (unpublished data). The difference in the bubble sizes between Jäsberg et al. at the current study is likely due to differences in the foam generation.

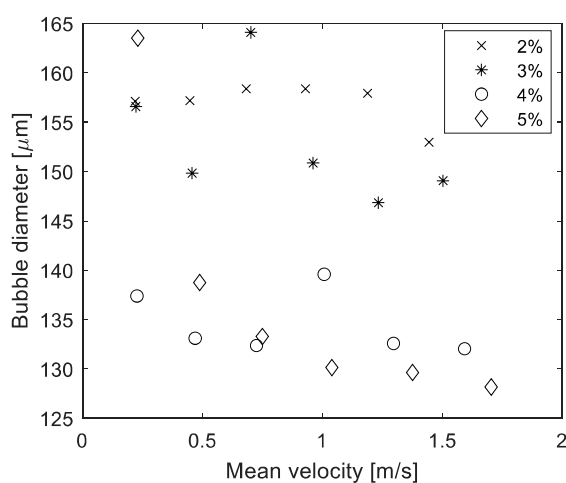


Figure 13 Bubble size as the function of mean velocity for different fiber consistencies. The measured bubble size has been converted to atmospheric pressure by using Eq. (4).

CONCLUSIONS

Fiber foams have unique rheological properties the study of which has only recently started. In this paper we looked at one interesting aspect; the effect of fibre consistency on the viscosity and slip behaviour of fiber foams. It was found that due to restricted interaction between the fibers the effect of increasing fiber consistency on foam viscosity is rather weak when compared water suspensions.

Moreover, the slip behavior was similar for all consistencies.

In the future there is a lot of scope for further studies relevant from both a practical and academic point of view: How does the fiber foam rheology depend on fiber type, fibre dimensions, air content, bubble size, temperature, and surfactant type and dosage? How do the various chemical additives and other materials used in paper and non-woven industry effect on the foam rheology?

REFERENCES

1. Hjelt, T. et al. *J. Disper Sci Technol* (2021), published online.
2. Lehmonen, J. et al. *Cellulose* 27, 1127–1146 (2020).
3. Kinnunen-Raudaskoski, K. et al. *Tappi J* 13, 9–19 (2014).
4. Dollet, B. & Raufaste C., *Phys Rep* 15, (8–9), 731–747 (2014).
5. Jäsberg, A., Selenius, P. & Koponen, A. *Colloid Surface A* 473, 147–155 (2015).
6. Jäsberg, A., Selenius, P. & Koponen, A. proceedings of 16th FRC symposium, 159–174, Oxford (2017).
7. Koponen, A. et al. *Nord. Pulp Pap. Res. J.* 33(3), 482–495 (2018).
8. Koponen, A. et al. *Tappi J* 18(8), 487–494 (2019).
9. Denkov, N. et al. *Soft Matter* 5, 3389–3408 (2009).
10. Mooney, M. *J. Rheol.* 2, 210–222 (1931).
11. Morrison, F. *Understanding Rheology*, New York, Oxford University Press (2001).
12. Calvert, J. *Int. J. Heat FL* 11, 236–241 (1990).
13. Koponen, A. *Cellulose* 27, 1879–1897 (2020).
14. Al-Qararah, A. et al. *Colloid Surface A* 467, 97–106 (2015).